Magnon Lifetimes on the Fe(110) Surface: The Role of Spin-Orbit Coupling

Kh. Zakeri,* Y. Zhang, T.-H. Chuang, and J. Kirschner
Max-Planck-Institut für Mikrostrukturphysik, Weinberg 2, 06120 Halle, Germany
(Received 16 January 2012; published 9 May 2012)

We provide direct experimental evidence which demonstrates that, in the presence of a large spin-orbit coupling, the lifetime, amplitude, group, and phase velocity of the magnons propagating along two opposite (but crystallographically equivalent) directions perpendicular to the magnetization are different. A real time and space representation reveals that magnons with the same energy (eigenfrequency) propagate differently along two opposite directions. Our findings can inspire ideas for designing new spintronic devices.

DOI: 10.1103/PhysRevLett.108.197205 PACS numbers: 75.30.Ds, 75.50.Bb, 75.70.Ak, 75.70.Rf

A key part of spintronics is concerned with effects, which are linked to the spin-dependent phenomena [1]. In 1960, Rashba proposed a formalism which nicely describes the existence of a spin-split band structure in wurtzite crystals [2]. Later on, Bychkov and Rashba showed that such a spin splitting can also occur in quantum wells [3]. The physical explanation of this spin splitting phenomenon is rather straightforward: in a semiconductor quantum well, if the potential well is asymmetric, the electrons move in an effective electric field, **E**, induced by the potential gradient of the quantum well. In the reference frame of the electron, this electric field transforms into an effective magnetic field, **B** [4], which causes a splitting in the energy levels of electrons with different spins. A similar effect is expected for the electrons in the absence of an inversion symmetry and in the presence of a large spin-orbit coupling [5]. A spin-split band structure has been observed on some metallic surfaces, where the inversion symmetry is broken [6] and could be explained in analogy to the conventional Rashba effect in semiconductor heterostructures [7–9]. The idea is further tailored to the surface alloys composed of heavy elements. The combination of strong spin-orbit interaction of the heavy elements with structural effects enhances the local potential gradients at the surface and thereby results in a large Rashba splitting [10]. The Rashba effect has been explored in detail in various systems, and even some spintronic devices are proposed based on this effect [11–14].

Magnons describe the collective and single particle excitations of a spin system. Although for small wave vectors they have a parabolic dispersion relation in ferromagnets (similar to the one of the free electrons), they are classified as bosonic quasiparticles (with a spin of $1\hbar$), unlike the electrons. One of the most interesting phenomena is the effect of the relativistic spin-orbit coupling on magnons as bosonic quasiparticles. Such an effect has not been explored in detail. Only recently, we have shown that the presence of the spin-orbit coupling in a spin system with broken inversion symmetry leads to an asymmetric magnon dispersion relation via the antisymmetric exchange interaction, known as Dzyaloshinskii-Moriya interaction (DMI) [15]. In principle, the spin-orbit coupling in the presence of the broken inversion symmetry may also influence the magnon lifetime and amplitude.

In this Letter, we will show that a large spin-orbit coupling in the presence of the broken space inversion symmetry does not only break the degeneracy of the magnon energy but also influences the magnon lifetime and amplitude (modulus). By probing the surface magnons along a direction lying exactly in the mirror symmetry plane of the film magnetization, we demonstrate that (i) in addition to the magnon energy, the magnon lifetime and amplitude are substantially affected by the presence of the spin-orbit coupling, and (ii) a careful analysis of the magnon spectra in real time and space reveals that the magnons with the same energy (eigenfrequency) but opposite propagation direction propagate differently in the presence of the spin-orbit coupling. Moreover, we will comment on the role of temperature on the observed effects within the temperature range of 10–300 K.

The magnon dispersion relation is measured along the $\bar{\Gamma}$-$\bar{H}$ direction of the surface Brillouin zone for a two-atomic-layer thick Fe film grown on W(110) at room temperature using spin-polarized electron energy loss spectroscopy (SPEELS) [16]. A two-atomic-layer thick Fe film on W(110) is ferromagnetic, with a Curie temperature far above room temperature [17]. It shows a strong uniaxial magnetic anisotropy with an easy axis along the $\langle\bar{1}10\rangle$ direction [17]. The dispersion relation is obtained by measuring the SPEEL spectra at different wave vectors [16,18]. The measurements were performed for the magnetization parallel to the $[\bar{1}10]$ and $[1\bar{1}0]$ directions. The results of such measurements are summarized in Fig. 1, demonstrating that the magnon dispersion relation is split into two branches for magnetization along two opposite directions. The dispersion relation is antisymmetric, meaning that the magnon energies for positive wave vectors are equal to the ones with negative wave vectors and opposite magnetization direction (or vice versa). In fact, the presence of the relativistic spin-orbit coupling in the absence of

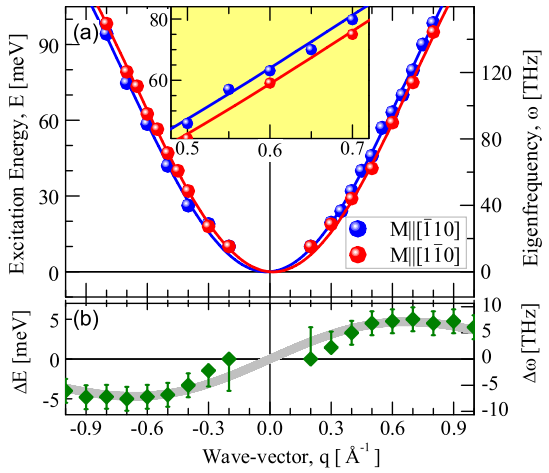

FIG. 1 (color online). (a) Magnon dispersion relation measured on a 2 ML Fe on W(110) at room temperature and for two different magnetization directions. The inset shows a magnified part of the graph for a smaller energy and wave-vector window. (b) The energy splitting defined as $\Delta E(q) = E_{M\|[\bar{1}10]}(q) - E_{M\|[1\bar{1}0]}(q)$ obtained from (a). The symbols represent the experimental results, while the solid lines represent the fits based on the extended Heisenberg spin Hamiltonian.

time reversal and space inversion symmetry breaks the degeneracy of the magnon energy and leads to a splitting of the magnon band structure. The asymmetric dispersion relation can be understood in terms of the antisymmetric DMI, which is a consequence of the spin-orbit coupling [15,19]. In such cases, the extended Heisenberg spin Hamiltonian (HSH) may be used to obtain the DM vectors. The extended HSH reads as $H = -\sum_{i\neq j} J_{ij}\mathbf{S}_i \cdot \mathbf{S}_j + \sum_{i\neq j}\mathbf{D}_{ij} \cdot \mathbf{S}_i \times \mathbf{S}_j - K\sum_i(\mathbf{S}_i \cdot \hat{e})^2$. The first term represents the symmetric exchange interaction with the isotropic exchange coupling constant J_{ij} between spins $\mathbf{S}_i$ and $\mathbf{S}_j$, the second term represents the antisymmetric DMI with the DM vectors $\mathbf{D}_{ij}$, and the last term accounts for the magnetic anisotropy energy in the system with an easy axis along $\hat{e}$ (K denotes the effective magnetic anisotropy energy constant). The solid lines in Fig. 1 are the fits based on the extended HSH given above. The fit parameters are $K = 0$, $J_1 = 7.5(5)$ meV, $J_2 = 4.5(3)$ meV, $|2D_1^x + \acute{D}_1^x| = 0.9(3)$ meV, and $|D_2^x| = 0.5(3)$ meV. The subscript 1(2) represents the nearest-neighbor (next-nearest-neighbor) interaction. D_1^x ($\acute{D}_1^x$) is the longitudinal component of the DM vector of the nearest neighbors in the same atomic plane (in the neighboring atomic plane). A detailed discussion and a comparison to the literature can be found in Ref. [15].

The splitting of the magnon band structure shown in Fig. 1 is very similar to the well-known Rashba effect observed for electrons in a two-dimensional electron gas or at metal surfaces [7–9]. Therefore, the effect may be called the "*magnon Rashba effect*" [20]. More importantly, we observed that the magnons' lifetimes are different when they propagate along opposite (but crystallographically equivalent) directions. Our experimental results are in line with the recent theoretical calculations based on the multiband Hubbard model [20]. The difference in the lifetime when the magnons propagate along opposite directions is a consequence of the spin-orbit coupling. The spin-orbit-induced damping is a well-known damping mechanism for small wave-vector magnons, in particular, in the case of the uniform ferromagnetic resonance mode ($q = 0$). As a simple model for the intrinsic ferromagnetic resonance damping, one may imagine the precession of the spin that is coupled to its orbital motion via the spin-orbit coupling. The orbital motion is perturbed by the lattice simultaneously and hence cannot follow the same phase anymore and it results in a damping. For high wave-vector magnons, the damping is mainly governed by dissipation into the Stoner states (known as *Landau* damping) [21]. In the case of Fe films on W(110), magnons are subjected to a large spin-orbit coupling coming mainly from the hybridization with the tungsten substrate. In such a case, a spin-orbit-induced damping is superimposed to the Landau type of damping. Since the time reversal inverts the angular and linear momentum, it inverts the spin-orbit contribution to the lifetime (the lifetime of magnons with $+M$, $+q$ is identical to the one of magnons with $-M$, $-q$). This is exactly what we observe in our experiment.

The spin Hamiltonian discussed above does not account for the magnons' lifetimes. In order to obtain detailed information on the magnons' lifetimes and amplitudes, one needs to perform a full intensity and broadening analysis of the excitations. For that, the SPEEL spectra are measured at a fixed scattering geometry and with exactly the same parameters (like incidence energy, beam current, and energy resolution) and only the sample magnetization is switched to the opposite direction. The experiment is designed such that the magnons propagate in the mirror symmetry plane of the magnetization. Since the magnon intensity depends on the scattering matrix elements, keeping the scattering geometry and experimental parameters unchanged during the experiment would avoid the effects caused by geometry on the electron scattering processes and thereby on the magnon intensity. Reversing the magnetization is equivalent to time inversion; therefore, one can reverse the magnon propagation direction only by reversing the direction of the magnetization. This approach opens a possibility to measure the magnons with positive and negative wave vectors without changing the scattering geometry. The SPEELS intensity spectra are recorded for different wave vectors. The difference spectra are obtained according to $I_{\mathrm{Diff.}} = I_\downarrow - I_\uparrow$ ($I_\downarrow$ and $I_\uparrow$ represent the intensity of the scattered electrons for the incidence of spin-down and spin-up electrons, respectively). The obtained SPEELS difference spectra are fitted with Voigt profiles [22], which then are plotted in Fig. 2 as a contour map (the

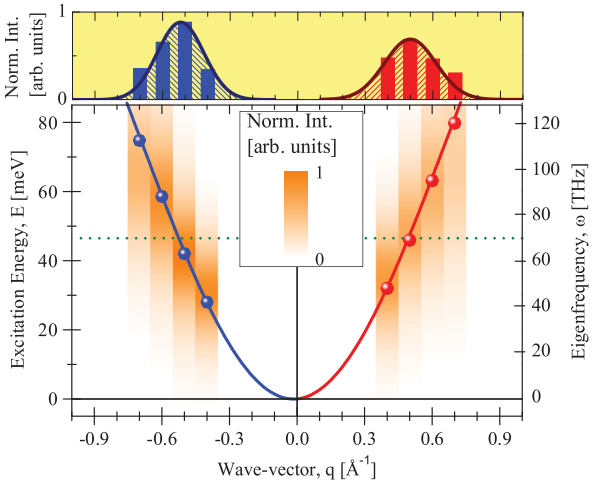

FIG. 2 (color). Magnon dispersion relation together with the intensity map. The negative branch is measured by reversing the magnetization. The SPEELS difference spectra are obtained based on $I_{\mathrm{Diff.}} = I_{\downarrow} - I_{\uparrow}$ after recording $I_{\downarrow}$ and $I_{\uparrow}$ spectra and are fitted with Voigt functions. The resulting curves are plotted as a contour map. The peak position is represented as solid circles. The solid line is a fit based on the extended Heisenberg spin Hamiltonian. The upper panel shows the intensity profile along the dotted line at $E = 46.5$ meV.

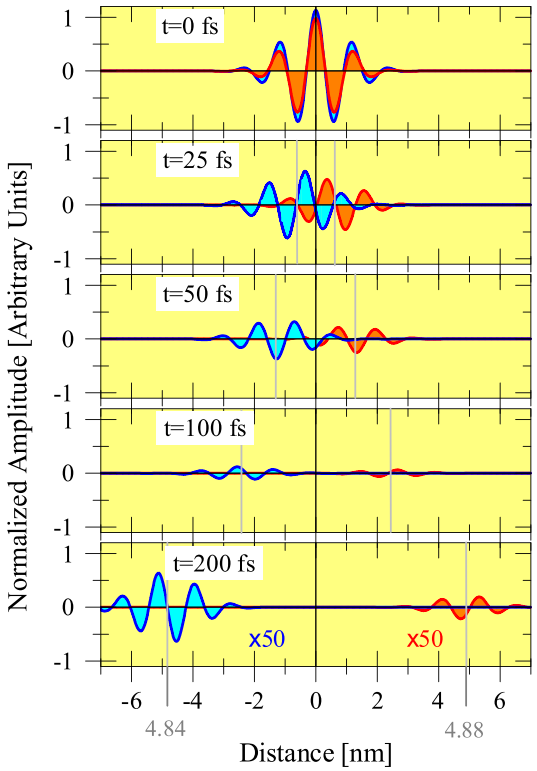

FIG. 3 (color online). A real time and space representation of the magnon wave packets. The wave packets start to propagate at $t = 0$, with the maximum amplitude at $x = 0$. The wave packet with smaller amplitude propagates along the [001] direction, and the one with larger amplitude propagates along the $[00\bar{1}]$ direction. The vertical gray lines indicate the center of the mass of the wave packets.

intensity is represented in the color scale). The excitation energies are shown as filled circles.

Now, we attempt to provide a real time and space representation of the magnons from our experimental data. This is essential because only then can we clearly see the consequences of the differences in the lifetime, amplitude, group, and phase velocity on the behavior of the magnon wave packets. An example is given for the magnons with an excitation energy of $E = 46.5$ meV. The distribution of magnon intensity in momentum space is obtained from the line profile at $E = 46.5$ meV. The profiles are shown in the upper panel of Fig. 2. We assume that the momentum distribution is a Gaussian distribution. Using the Fourier transform, one can have direct access to the real space representation of the magnons. For the magnons with an energy of $E = 46.5$ meV, the wave vectors are $+0.50$ Å^{-1} and -0.52 Å^{-1}. The corresponding wavelengths are about 12.6 Å and 12.1 Å, respectively. Note that, in the absence of relativistic effects, the absolute values of the wave vectors (wavelengths) for the positive and negative branches have to be exactly the same. The difference in the absolute value of the wave vectors (wavelengths) is a direct consequence of the spin-orbit coupling. The real time and space representation of the magnons is presented in Fig. 3 (see the animated movie in the Supplemental Material [23]). The magnon wave packet starts to propagate at $t = 0$, with the maximum amplitude at $x = 0$. The lifetime of the magnons in itinerant ferromagnets is usually very short. It is defined as the time in which the amplitude of the magnon wave packet is reduced by a factor of $1/e$. The values obtained at $E = 46.5$ meV for positive and negative wave vectors are $\tau_{+} \approx 37 \pm 5$ fs and $\tau_{-} \approx 45 \pm 5$ fs, respectively. The short wavelength together with the short lifetime compress the magnon's wave packet such that it contains only a few oscillations in space (see Fig. 3). The group velocity, $v_g = \partial\omega/\partial q$ ($\omega = E/\hbar$ is the eigenfrequency and q is the wave vector), is obtained from the slope of the dispersion curve at the given energy ($E = 46.5$ meV) and wave vectors ($q = +0.50$ Å^{-1} and -0.52 Å^{-1}). Since the dispersion relation is asymmetric, the group velocity is different for the magnons propagating along two opposite directions. For the ones that are propagating along the [001] direction (the ones with $q = +0.50$ Å^{-1}), it is $v_g = 24.4$ km/s, and, for the ones propagating along the $[00\bar{1}]$ direction (the ones with $q = -0.52$ Å^{-1}), it is about $v_g = -24.2$ km/s. The differences in the group velocity, lifetime, and amplitude lead to a different propagation behavior for the magnons along two opposite directions. Figure 3 demonstrates that after 200 fs the magnon's wave packet, which is propagating along the [001] direction, propagates 48.8 Å and is strongly damped but the one which is propagating along the $[00\bar{1}]$ direction propagates 48.4 Å. The extrapolation of

our results to $q = 0$ reveals that the uniform mode with zero wave vector possesses a finite group velocity of about $v_g(q = 0) \approx 1$ km/s. The phase velocity can be obtained using the simple expression $v_p = E/q$, which results in $v_p = 14.4$ km/s for the magnons with an energy of 46.5 meV and $q = 0.50$ Å^{-1}. It is about -13.4 km/s for the magnons with an energy of 46.5 meV and $q = -0.52$ Å^{-1}. The phase velocity is smaller than the group velocity, meaning that the magnon wave packets disperse during the propagation (see Fig. 3 and [23]).

Now, we comment on the temperature effects. The experiments performed at 10 K reveal that the splitting of the magnon band structure and the spin-orbit-induced modifications of the lifetime and amplitude, discussed above, do not depend strongly on temperature. The splitting in the energy observed for the wave vector of ± 0.5 Å^{-1} is about $\Delta E = 6 \pm 2$ meV at 10 K, which is very close to the value measured at 300 K. The absolute values of magnon energies measured at low temperatures are found to be slightly larger than the ones measured at 300 K. This reflects mainly the temperature dependence of the effective exchange coupling (or exchange stiffness). The negligible temperature dependence of this effect might be due to the fact that the Curie temperature of the system is far above the measured temperature window [17].

The effect discussed above may be used to propose spintronic devices, since it is not restricted to the Fe/W (110) system. The basic functionality of such a device would be somehow similar to the ones that are proposed based on the conventional Rashba effect [1,11–14], but with considering the fact that magnons are basically different from electrons. The simplest device, based on this principle, can be imagined as follows: One excites the transversal surface magnons (those that are propagating perpendicular to the magnetization) on a ferromagnetic surface. Simultaneously, two wave packets will propagate to opposite directions. Because of the spin-orbit-induced effects, the wave packet which is propagating towards the left gate possesses a larger amplitude and lifetime, while the one that is propagating towards the right gate will die out quickly. When the magnon wave packet arrives at the left gate, it can be detected. At the same time, no magnon signal can be detected by the other gate. The switching of this state to a state in which the right gate detects a signal and no signal arrives at the left gate can be realized just by reversing the magnetization of the ferromagnet (see the text in the Supplemental Material [23]). Since the magnons discussed here have wavelengths of a few nanometers, they would allow signal processing at the nanometer scale, which is essential for such small devices. However, the suggestion and realization of such devices require detailed knowledge of the basic concepts of the effect.

In conclusion, we showed that, in addition to the magnons' energy, their lifetime and amplitude are also modified by spin-orbit coupling, when they propagate along two opposite directions perpendicular to the magnetization. The differences in the lifetime, amplitude, and group velocity lead to a substantial difference in the magnon propagation behavior along two opposite (but crystallographically equivalent) directions. The spin-orbit-induced effects on magnon band structure, lifetime, and amplitude are found to be nearly temperature-independent within the temperature range of 10–300 K. In addition to the fact that our results manifest the relativistic spin-orbit effects on spin excitations, which will provide a deeper understanding of magnetism on the nanoscale, they may inspire new ideas for designing new spintronic devices based on these effects.

*Corresponding author
zakeri@mpi-halle.de

[1] S. A. Wolf, D. D. Awschalom, R. A. Buhrman, J. M. Daughton, S. von Molnár, M. L. Roukes, A. Y. Chtchelkanova, and D. M. Treger, Science **294**, 1488 (2001).
[2] E. I. Rashba, Sov. Phys. Solid State **2**, 1109 (1960).
[3] Yu. A. Bychkov and E. I. Rashba, JETP Lett. **39**, 78 (1984).
[4] H. Chapman and C. A. R. Sa de Melo, Nature (London) **471**, 41 (2011).
[5] R. Winkler, *Spin-Orbit Coupling Effects in Two-Dimensional Electron and Hole Systems* (Springer, New York, 2003).
[6] S. LaShell, B. A. McDougall, and E. Jensen, Phys. Rev. Lett. **77**, 3419 (1996).
[7] J. Henk, A. Ernst, and P. Bruno, Phys. Rev. B **68**, 165416 (2003).
[8] O. Krupin, G. Bihlmayer, K. Starke, S. Gorovikov, J. E. Prieto, K. Döbrich, S. Blügel, and G. Kaindl, Phys. Rev. B **71**, 201403(R) (2005).
[9] G. Bihlmayer, Yu. M. Koroteev, P. M. Echenique, E. V. Chulkov, and S. Blügel, Surf. Sci. **600**, 3888 (2006).
[10] C. R. Ast, J. Henk, A. Ernst, L. Moreschini, M. C. Falub, D. Pacile, P. Bruno, K. Kern, and M. Grioni, Phys. Rev. Lett. **98**, 186807 (2007).
[11] S. Datta and B. Das, Appl. Phys. Lett. **56**, 665 (1990).
[12] T. Koga, J. Nitta, H. Takayanagi, and S. Datta, Phys. Rev. Lett. **88**, 126601 (2002).
[13] H. C. Koo, J. H. Kwon, J. Eom, J. Chang, S. H. Han, and M. Johnson, Science **325**, 1515 (2009).
[14] I. M. Miron, G. Gaudin, S. Auffret, B. Rodmacq, A. Schuhl, S. Pizzini, J. Vogel, and P. Gambardella, Nature Mater. **9**, 230 (2010).
[15] Kh. Zakeri, Y. Zhang, J. Prokop, T.-H. Chuang, N. Sakr, W. X. Tang, and J. Kirschner, Phys. Rev. Lett. **104**, 137203 (2010).
[16] H. Ibach, D. Bruchmann, R. Vollmer, M. Etzkorn, P. S. Anil Kumar, and J. Kirschner, Rev. Sci. Instrum. **74**, 4089 (2003).
[17] H. J. Elmers, Int. J. Mod. Phys. B **9**, 3115 (1995).
[18] W. X. Tang, Y. Zhang, I. Tudosa, J. Prokop, M. Etzkorn, and J. Kirschner, Phys. Rev. Lett. **99**, 087202 (2007).

[19] L. Udvardi and L. Szunyogh, Phys. Rev. Lett. **102**, 207204 (2009).
[20] A. T. Costa, R. B. Muniz, S. Lounis, A. B. Klautau, and D. L. Mills, Phys. Rev. B **82**, 014428 (2010).
[21] P. Buczek, A. Ernst, and L. M. Sandratskii, Phys. Rev. Lett. **106**, 157204 (2011).
[22] The choice of the Voigt function is based on the fact that the measured SPEELS spectra are a convolution of a Lorentzian line shape with a Gaussian distribution, caused by instrumental broadenings.
[23] See Supplemental Material at http://link.aps.org/supplemental/10.1103/PhysRevLett.108.197205 for detailed information.